Seasonal dynamics in diatom and particulate export fluxes to the deep sea in the Australian sector of the southern Antarctic Zone

Andrés S. Rigual-Hernández, Thomas W. Trull, Stephen G. Bray, Ivia Closset, Leanne K. Armand

HAL Id: hal-01103113

https://hal.sorbonne-universite.fr/hal-01103113v1

Submitted on 14 Jan 2015

1   **Seasonal dynamics in diatom and particulate export fluxes to the deep sea in the**

2   **Australian sector of the southern Antarctic Zone**

3   Andrés S. Rigual-Hernandez[1*], Thomas W. Trull[2,3], Stephen G. Bray[2], Ivia Closset[4],

4   Leanne K. Armand[1].

5   1 Department of Biological Sciences, Macquarie University, North Ryde, NSW 2109,

6   Australia

7   2 Antarctic Climate and Ecosystems Cooperative Research Centre, University of

8   Tasmania, Hobart, Tasmania 7001, Australia

9   3 CSIRO Oceans and Atmosphere Flagship, Hobart, Tasmania 7001, Australia

10   4 Sorbonne Universités (UPMC, Univ Paris 06)-CNRS-IRD-MNHN, LOCEAN

11   Laboratory, 4 place Jussieu, F-75005 Paris, France

12

13   *Corresponding author (andres.rigualhernandez@mq.edu.au)

14

16

17   **Abstract**

18   Particle fluxes were recorded over a one-year period (2001-02) in the southern Antarctic

19   Zone in the Australian Sector of the Southern Ocean. Here, we present the results on the

20   seasonal and vertical variability of biogenic particle and diatom valve fluxes. Total mass

21   and diatom fluxes were highly seasonal, with maxima registered during the austral

22   summer and minima during winter. Biogenic opal dominated sedimentation, followed

23   by carbonate, and very low levels of organic carbon (annual average 1.4%). The strong

24   correlation between opal and organic carbon at both depth levels suggests that a

25   significant fraction of organic matter exported to the deep sea was associated with

diatom sedimentation events. Seasonal diatom fluxes appear driven principally by changes in the flux of *Fragilariopsis kerguelensis*. The occurrence of the sea-ice affiliated diatoms *Fragilariopsis cylindrus* and *Fragilariopsis curta* in both sediment traps is considered to correspond to the sedimentation of a diatom bloom advected from an area under the influence of sea ice. Highest fluxes of the subsurface-dwelling species *Thalassiothrix antarctica* registered at the end of the summer bloom were linked to a drop of the light levels during the summer-autumn transition. This study provides the first annual observation on seasonal succession of diatom species in the Australian sector of the Antarctic Zone, and corresponds, in terms of magnitude and seasonality of diatom fluxes, to those in neighbouring sectors (Pacific and eastern Atlantic).

1. Introduction

Diatoms are unicellular algae with an absolute requirement for silicic acid to form their frustules. They constitute a major component of phytoplankton communities, being responsible for ~40% of all marine carbon fixation (Nelson et al., 1995). Diatoms are the main contributors to the silica-rich deposits in deep-sea sediments and are thought to influence the present and past global climate via their influence on the biological pump of CO_2 from the atmosphere into the ocean interior (Nelson et al., 1995; Sarmiento et al., 1998; Matsumoto et al., 2002). The composition of phytoplankton communities and abundance of diatoms within them are related to specific ecological parameters of the water masses where they live (e.g., temperature, sea-ice cover and nutrient availability), and hence in the case of diatoms, their frustules can be used as biotic proxies for palaeoenvironmental and palaeoceanographic reconstructions.

49   In order to evaluate the role of diatoms in the biological pump and the cycling of

50   silicon, it is essential to thoroughly understand their ecology and the processes that the

51   living biocoenoses undergo from their initial production in the euphotic zone to their

52   eventual preservation in the ocean sediments (e.g. Varela et al., 2004; Grigorov et al.,

53   2014). This knowledge is also required to validate paleorecontructions based on the

54   diatom sedimentary record (e.g. Leventer et al., 1993; Taylor and Sjunneskog, 2002;

55   Armand and Leventer, 2010).

56   The Southern Ocean is regarded as having one of the highest diatom biomasses of the

57   global ocean. Despite its high-nutrient low chlorophyll (HNLC) regime, massive diatom

58   blooms occur every year during spring and summer associated with specific areas, such

59   as oceanographic fronts (e.g. Honjo et al., 2000; Moore and Abbott, 2002), coastal areas

60   of Antarctica (e.g. Wefer et al., 1988, Bathmann et al., 1991; Arrigo et al., 1999) and the

61   retreating sea ice edge (e.g. Smith and Nelson, 1986; Sullivan et al., 1988). As a result

62   of this relatively high diatom productivity (Pondaven et al., 2000), large amounts of

63   biogenic silica accumulate in the Southern Ocean sediments, mainly south of the

64   Antarctic Polar Front (APF), where about 30% of the global opal marine accumulation

65   occurs (Tréguer and De la Rocha, 2013).

66   Moored sediment traps are one of the few available tools for monitoring particle fluxes

67   in the open ocean over extended periods of time. They provide a means to determine the

68   magnitude and timing of phytoplankton blooms, document species succession and

69   estimate the remineralization of labile components throughout the water column. The

70   use of sediment traps has contributed significantly to our understanding of diatom

71   ecology in the Southern Ocean and coastal Antarctic systems (e.g. Leventer and

72   Dunbar, 1987; Fischer et al., 1988; Leventer and Dunbar, 1996; Abelmann and

73   Gersonde, 1991; Ishikawa et al., 2001; Suzuki et al., 2001; Pilskaln et al., 2004;

Ichinomiya et al., 2008; Romero and Armand, 2010). However, these studies are scattered in space and time, and large regions of the Southern Ocean, including the Australian Sector, remain undocumented.

During the Australian multidisciplinary ACE CRC SAZ Project (Trull et al., 2001a), the main hydrological zones of the Australian sector of the Southern Ocean were instrumented with sediment trap mooring lines. The central goal of this experiment was to determine the origin, composition and fate of particulate matter transported to the ocean interior. This research yielded important results, including the demonstration that particulate organic carbon (POC) export in the Southern Ocean is similar to the global ocean median (Bray et al., 2000; Trull et al., 2001b).

Here, as part of the ACE CRC SAZ project, we report on the biogenic particle fluxes registered by two sediment traps deployed in the southern Antarctic Zone (60° 44.43´S; 139°E 53.97´S) over a year (November 2001 to September 2002) in order to (1) document the magnitude, composition and seasonal distribution patterns of the settling particle fluxes, with particular focus on diatoms and their specific composition; and (2) assess the effects of dissolution and physical processes in the water column on the diatom assemblage composition by comparing the assemblages registered by the 2000 and 3700 m sediment traps. An improved understanding of diatom ecology and changes that the diatom assemblages undergo during their sinking through the water column should lead to a better interpretation of proxy records in the Southern Ocean.

1.1. Oceanographic setting

The Antarctic Circumpolar Current (ACC) flows eastward around Antarctica driven by strong westerly winds connecting the Pacific, Atlantic and Indian Oceans. Several circumpolar jets or fronts divide the ACC into distinct zones (Fig. 1a), each one

characterized by specific hydrological and biochemical properties (Orsi et al., 1995). The fronts coincide with strong current cores of the ACC defined by contours of sea surface height (SSH). Each of these fronts consists of multiple branches or filaments, where their position varies rapidly over time (Sokolov and Rintoul, 2002, 2007 and 2009a, b). From north to south, these fronts and zones are the Subtropical Front (STF), the Subantarctic Zone (SAZ), the Subantarctic Front (SAF), the Polar Frontal Zone (PFZ), the Polar Front (PF), the Antarctic Zone (AZ) and the Southern ACC Front (SACCF) (Sokolov and Rintoul, 2009a, b).

The surface waters of the Australian sector of the Southern Ocean are nitrate and phosphate rich and their concentrations remain fairly uniform across the ACC (Bostock et al., 2013). In contrast, silicic acid (Si) content shows a marked south to north gradient. Highest Si concentrations are reached south of the Polar Front Zone (up to 70 μM), whereas the Subantarctic Zone waters exhibits low Si values (1 to 5 μM) (Coale et al., 2004; Bostock et al., 2013). Despite the relatively high macronutrient concentrations, Southern Ocean surface waters are often characterized by relatively low phytoplankton biomass. Light limitation related to deep mixing (Sakshaug and Holm-Hansen, 1984) and extremely low concentrations of trace metals such as iron (De Baar et al., 1995; Johnson et al., 1997; Fitzwater et al., 2000; Martin et al., 1990; Boyd et al., 2000) seem to be the main causes for this "high-nitrate, low-chlorophyll" (HNLC) regime.

Sea ice seasonality off East Antarctica is considered linked to patterns of oceanic currents, which in turn are related to sea floor topography (Massom et al., 2013). Seasonal sea-ice advance occurs from early autumn through early spring followed by retreat from late spring through summer (Comiso et al., 1984; Kimura and Wakatsuchi, 2011; Massom et al., 2013).

124   Our study site, station 61 S (60° 44.43´S; 139°E 53.97´S), is located within the southern

125   Antarctic Zone (AZ-S; Parslow et al., 2001), between the southern branch of the PF

126   (59°S) and the southern front of the SAACF (Rintoul and Bullister, 1999; Rintoul and

127   Sokolov, 2001). The mooring site is within the same region where the first open-ocean

128   iron enrichment experiment in the Southern Ocean (Southern Ocean Iron Release

129   Experiment - SOIREE) was conducted (Boyd et al., 2000) and can be considered

130   representative of the region between the PF and the SACCF (between 54°S and 62°S)

131   (Trull et al., 2001c). Despite surface waters rich in macronutrients (i.e. silicate,

132   phosphate and nitrate), the algal biomass accumulation is considered low (<0.5 µg/L)

133   (Parslow et al., 2001; Popp et al., 1999; Trull et al., 2001c). Copepods, mainly large

134   calanoid copepodites, dominate the zooplankton community at the study site. Grazing

135   pressure is considered low (<1% of the phytoplankton standing stock removed per day)

136   and is thought not to greatly influence the development of the annual bloom (Zeldis,

137   2001). Very low iron concentrations (0.1-0.2 nM; Sohrin et al., 2000; Boyd et al., 2000)

138   appear to be responsible for the low primary production. The study area is far from the

139   influence of coastal waters and just north of the maximum winter sea-ice extent (Fig.

140   1b; Massom et al., 2013).

141

142   **2. MATERIAL AND METHODS**

143   **2.1 Field experiment**

144   Site 61 S was instrumented with a mooring line equipped with three McLane Parflux

145   time series sediment traps (Honjo and Doherty, 1988) placed at 1000, 2000 and 3700 m

146   depth in a water column of 4393m (Fig. 1c). Each trap was paired with an Aanderaa

147   current meter and temperature sensor. The trap sampling cups were filled with a

148   buffered solution of sodium tetraborate (1 g L^{-1}), sodium chloride (5 g L^{-1}), strontium

149 chloride (0.22 g L^{-1}), and mercury chloride (3 g L^{-1}). Cup rotation intervals were

150 synchronized between traps and were established based on anticipated mass fluxes. The

151 shortest sampling intervals were 8 days and correspond with the austral summer and

152 autumn, whereas the longest interval was 55 days corresponding with austral winter

153 (Table 1). No samples were recovered from the shallowest trap owing to equipment

154 malfunction. The two deeper traps completed their collection sequence as programmed

155 without any instrumental failures providing a continuous time-series for 317 days

156 (November 30, 2001 to September 29, 2002) divided into 21 collecting intervals. Owing

157 to the low particle fluxes registered at the onset and end of the experiment insufficient

158 material remained for diatom analysis of cup 1 of the 2000 m trap and cups 1, 2, 19, 20

159 and 21 of the 3700 m trap (Table 1). After recovery, sediment trap cups were removed,

160 capped on board and stored at 4°C in the dark until they were processed. The original

161 samples were sieved through a 1mm nylon mesh in order to remove the largest

162 swimmers, and only the fraction <1 mm was analyzed. Then, they were split into 10

163 equal fractions using a McLane WSD-10 wet-sample divider. One complete split was

164 used for microplankton analysis. A detailed description of the geochemical analytical

165 procedures is given by Trull et al. (2001b) and Bray et al. (2000). Component fluxes are

166 reported for individual cups along with average values over the collection or

167 deployment period for each component (Table 1). As the collection period was shorter

168 than a calendar year, annual mean estimates were determined and are presented in Table

169 1. These annual estimates take into account the fact that the unobserved days occurred

170 in winter when fluxes were low, and were obtained by using the flux for the last winter

171 cup (#21 in 2002) to represent mean daily fluxes during the unobserved period.

172 In order to investigate the correlation between time series, a correlation matrix was

173 calculated (Table 2).

174

2.2 Siliceous microplankton sample preparation and analysis

Each diatom fraction sample was refilled with distilled water to 40 ml, from which 10 ml was subsampled and buffered with a solution of sodium carbonate and sodium hydrogen carbonate (pH 8) and kept refrigerated for future calcareous nannoplankton analysis. The remaining 30 ml was treated with hydrogen peroxide, potassium permanganate and concentrated hydrochloric acid in order to clean the sample of organic matter and calcareous components following the methodology of Romero et al. (1999, 2000). The resulting sediment slurry was stored in bottles filled with distilled water. Microscopic slides were prepared following the decantation method outlined by Flores and Sierro (1997). This method produces random settling of the diatoms for quantitative microscopic purposes. The dried cover-slip was permanently mounted onto a glass slide with Norland optical adhesive 61 mounting medium (Refractive index: 1.56).

Qualitative and quantitative analyses were performed using a Olympus BH-2 compound light optical microscope at 1000x magnification with phase-contrast illumination. A minimum of 400 specimens were counted per sample. Each diatom valve was identified to the lowest taxonomic level possible. Scanning Electron Microscope observations of selected samples were used to verify taxonomic identifications made with the LM. The recommendations of Schrader and Gersonde (1978) were used as a basis for the counting of diatom valves. We did not include the counts of the girdle bands of *Dactyliosolen antarcticus* in the determination of relative abundances.

The microplankton counts were transformed into daily fluxes of specimens m^{-2} d^{-1} following the formula of Sancetta and Calvert (1988) and Romero et al. (2009):

198

8

$$F = \frac{Nx \left(\frac{A}{a}\right) x\, V \, x\, S}{d \; x \; T}$$

199

200 where "F" is the daily flux of specimens, *N* the number of specimens, "A" the total

201 area of a Petri dish, "a" the analysed area, "V" the dilution volume, "S" the split of the

202 cup, "d" the number of days of collection and "T" the aperture area of the sediment trap.

203 The diatom species diversity was estimated applying Shannon's diversity index (H´) to

204 the relative abundance data (H´= - $\sum p_i \log_2 p_i$, where p = n1/N, n1 = number of

205 specimens of one taxon and N the total number of specimens). Large values of H

206 indicate greater diversity.

207 The annualized diatom valve flux for the 2000 m sediment trap was estimated following

208 the same procedure as for the component fluxes (Table 1).

209 The temporal overlap of diatom fluxes between 2000 m and the 3700 m traps occurred

210 between December-May (172 days) (Table 1). This overlap was used to estimate the

211 sinking velocities of diatom valves and to track the alteration of settling diatom

212 assemblages between traps. The sinking settling velocities for the main diatom taxa

213 were calculated from the time lag between associated peaks in both traps and the

214 vertical distance between traps. We used a squared-chord distance as the metric for

215 assessing the similarity between the diatom assemblages of both traps (Ortiz and Mix,

216 1997). Squared chord distance values can range between 0.0 and 2.0, with 0.0 indicating

217 identical proportions of species within the assemblages being compared.

218

219 **2.3 Satellite imagery, meteorological and oceanographic data**

220 Weekly mean sea surface temperature (SST) data for the period 2001 to 2002 was

221 extracted from the NOAA Optimum Interpolation Sea Surface Temperature Analysis

222 database (Reynolds et al., 2002). The monthly averages of the upper 300 m thermal

223   structure for the 2001–2002 period (Fig. 2) were obtained for the sampling location

224   from the World Ocean Atlas 2009 (Locarnini et al., 2010). The maximum weekly SST

225   mean during the field experiment was 2.94 °C degrees occurring in March 2002,

226   whereas the minimum was 0.12 °C at the beginning of October 2002. Changes of the

227   weekly mean SST mirrored the seasonal changes in the vertical structure of the water

228   column temperature profile. A pattern of stratification during austral summer months

229   and vertical homogeneity in autumn and winter was noted during the field experiment

230   (Fig. 2).

231   Satellite-derived monthly chlorophyll-*a* concentration and photosynthetically active

232   radiation (PAR) estimates were obtained from NASA's Giovanni program (Acker and

233   Leptoukh, 2007) (Fig. 2). The pigment concentration record was then used as a proxy

234   for surface algal biomass accumulation. The overall chlorophyll-*a* levels were low

235   (0.07-0.30 mg/m^3) and similar to previous observations in the study area (Trull et al.,

236   2001c). The increase in the algal biomass commenced in September 2001 and reached

237   its highest levels in November 2001, coinciding with a maximum in the insolation

238   levels (Fig. 2). Pigment concentration declined through summer and reached its lowest

239   levels in autumn and winter (March to August 2002).

240

241   **3. RESULTS**

242   **3.1 Bulk composition**

243   Total fluxes of particulates at both traps were highly seasonal, with maxima registered

244   during the austral summer (up to 1151 mg m^{-2} d^{-1} at 2000 m and 1157 mg m^{-2} d^{-1} at 3700

245   m) and almost negligible fluxes during winter (up to 42 mg m^{-2} d^{-1} at 2000 m and below

246   detection limits at 3700 m) (Fig. 2). The fluxes of total particulates at 2000 and 3700 m

247   depth showed similar seasonal variations and were closely correlated (R^2 = 0.82; Fig.

248 4). Particulate fluxes were slightly higher at 2000 m (261 ± mg m^{-2} d^{-1} = deployment

249 average ± standard deviation) than at 3700 m (216 ± 337 mg m^{-2} d^{-1}). Biogenic silica

250 (SiO$_2$) was the dominant bulk component, regardless of the sampling period or depth

251 (deployment average = 76% at 2000 and 78% at 3700 m). The highest relative

252 contribution of opal was registered from the end of summer through early-autumn at

253 both depths (Table 1). Secondary contributors were carbonate (CaCO$_3$) (7% at 2000 m

254 and 9% at 3700 m) and particulate organic carbon (POC) (1.4% at 2000 m and 1.2% at

255 3700 m). The relative concentration of carbonate and POC was at its highest in austral

256 spring and summer (Table 1). The fluxes of all components were closely correlated. The

257 results of the correlation matrix are given in Table 2. Total mass flux showed a strong

258 correlation with POC at both sediment traps (R^2 = 0.86 at 2000 m and R^2 = 0.87 at 3700

259 m). BSiO$_2$ fluxes were also highly correlated with POC at both depths (R^2 = 0.83),

260 whereas CaCO$_3$ and POC fluxes exhibited the lowest values (R^2 = 0.24 at 2000 m and

261 R^2 = 0.63 at 3700 m).

262 The molar POC/PN ratios were relatively low (Table 1), and thus similar to surface

263 Southern Ocean particles and phytoplankton (Copin-Montegut and Copin-Montegut,

264 1983).

265 **3.2 Composition of the biogenic opal fraction**

266 The biogenic opal fraction was composed of diatoms, silicoflagellates, radiolarians and

267 the dinoflagellate *Actiniscus pentasterias*. Diatoms were, numerically, the dominant

268 siliceous plankton group registered by the traps with a mean flux between 67 x 10^6 and

269 76 x 10^6 valves m^{-2} day^{-1} at 2000 m (annualized mean and deployment average,

270 respectively). Mean diatom flux at the 3700 m trap yielded higher values (deployment

271 average = 132 x 10^6 valves m^{-2} day^{-1}) due to the lower sampling duration (172 days)

272 over the winter season (Table 1). Silicoflagellates and radiolarians were three and four

273 orders of magnitude lower than diatoms (not shown), whereas only one specimen of *A.*

274 *pentaserias* was indentified in the lower trap. At both depth levels, total diatom fluxes

275 showed strong seasonal variations that closely followed total mass seasonality with

276 Pearson correlation coefficients of r = 0.88 for 2000 m and r = 0.81 for 3700 m (Fig. 4).

277 Diatom frustules from 61 taxa were identified over the entire experiment and are listed

278 in Table 3 together with their relative contribution for the whole sampling period. The

279 seasonal changes in the diatom flux and main species at mooring site 61°S are plotted in

280 Figure 5.

281 Diversity index values (H´) followed the same seasonal trend as total diatom flux at

282 both depths, with highest values registered during austral summer and lowest during

283 winter (Fig. 5). The squared-chord distance between the sediment trap diatom

284 assemblages at 2000 and 3700 m was 0.003, indicating highly similar proportions of

285 species within depths.

286 The dominant species of the diatom assemblage was *Fragilariopsis kerguelensis* with a

287 mean flux between 53 x 10^6 and 60 x 10^6 valves m^{-2} day^{-1} at 2000 m (annualized mean

288 and deployment average, respectively). This species contribution ranged from 37% to

289 96% of the total assemblage at 2000 m (average relative contribution for the

290 overlapping period between traps = 72%; Table 3) and from 31% to 82% at 3700 m

291 (average relative contribution for the overlapping period between traps = 68%) (Table

292 3). The diatom flux peaks at both depths can be attributed to an increased flux of *F.*

293 *kerguelensis*, with exception to a peak in late January at 2000 m when *Fragilariopsis*

294 *pseudonana* dominated the settling assemblage (39%). Secondary contributors to the

295 diatom assemblage at 2000 and 3700 m were *Thalassiosira lentiginosa* (average relative

296 contribution for the overlapping period between traps = 5% and 7%, respectively),

297 *Thalassiosira gracilis* var. *gracilis* (6% and 7%), *Fragilariopsis separanda* (3% and

298   2%), *Fragilariopsis pseudonana* (4% and 1%), *Fragilariopsis rhombica* (2% and 2%),

299   *Fragilariopsis curta* (1% and 1%) and *Azpeitia tabularis* (1% and 1%) (Table 3 and Fig.

300   5). It is worth noting that some large and/or entangled frustules of some diatom taxa,

301   such as *Thalassiothrix* (Hallegraeff, 1986), could have been be retained in the 1 mm

302   screen mesh, and therefore, underrepresented in this study.

303   Scanning electron microscope (SEM) pictures of some of the most relevant taxa are

304   shown in Fig. 6.

305

306   **3.3 Diatom settling velocities**

307   The calculation of the sinking velocities of the main diatom taxa was only possible for

308   the "particle bloom" period, i.e. from December to March, when distinct peaks were

309   registered in both sediment traps (Fig. 5). The precision of the calculations is limited by

310   the duration of the sampling intervals during this period (8 days). The majority of the

311   taxa exhibited an offset of a single sampling interval (8 days) between the 2000 and

312   3700 m traps, suggesting and average settling speed of 210 m d^{-1}.

313

314   **4. DISCUSSION**

315   **4.1 Quality check of downward particle fluxes**

316   The use of sediment traps has greatly enhanced our understanding of particle transfer in

317   open ocean environments. However, laboratory and field experiments have shown that

318   the measurement of downward particle fluxes can be subject to several hydrodynamic

319   biases (e.g. Gardner, 1980; Baker et al., 1988, Yu et al., 2001). Therefore, an assessment

320   of the trapping efficiency is needed prior to interpreting the results of any sediment trap

321   experiment.

322   Our mooring line at site 61°S was maintained taut by the distribution of floats along the

323   line and at the mooring head. Measured mean current speeds at both trap levels were

324   always lower than 10 cm s^{-1} that is, as a rule of thumb, considered the threshold at

325   which trapping efficiency decreases significantly (e.g. Baker et al., 1988, Honjo et al.,

326   1992, Yu et al., 2001, Heussner et al., 2006). On the basis of global comparisons, these

327   conditions suggest that fluxes registered by the traps were unlikely to be significantly

328   biased by under- or over-trapping (Honjo. 1996; Yu et al., 2001).

329   **4.2 Variability of total mass flux and composition of particles**

330   The seasonal variability of the vertical particle transfer at site 61°S appears principally

331   controlled by seasonal changes in the euphotic zone productivity. A significant increase

332   in chlorophyll-*a* concentration from October 2001, approximately two months before

333   any significant warming or stratification occurs (Fig. 2), is in line with an increase in

334   incident insolation from the beginning of spring. Taking into account that pigment

335   concentration at the sea surface reached its highest levels during November 2001 (Fig.

336   2), and that maximum total particle and diatom fluxes were registered at the beginning

337   of January 2002 (Figs 3 and 5), a time lag of about two months between peak

338   production in the surface waters and onset of particle export in the study area can be

339   assumed. This feature is in agreement with the observations of Buesseler et al. (2001) in

340   the Pacific Sector of the Southern Ocean who reported a similar delay in the delivery of

341   the surface bloom to the ocean interior. Contrastingly, algal biomass reached its annual

342   minimum during the austral winter (June-September) (Fig. 2) and very low particle and

343   diatom export fluxes were registered by the traps (Fig. 3 and 5). These low chlorophyll-

344   *a* concentration and flux values appear to be driven by two factors: (i) insufficient

345   sunlight as a result of the low solar angle and shortened day length that reduced the

346   ability to increase biomass and (ii) intense vertical mixing that transported

14

347   phytoplankton below their critical depth, i.e. depth at which the rate of photosynthesis

348   equals the rate of respiration (Fig. 2).

349   In terms of particle composition, silica-rich and carbonate-poor particulate fluxes

350   registered by the traps mirrored the dominance of diatoms in the waters south of the

351   Antarctic Zone, south of Tasmania. The composition of the settling material is

352   consistent with that of the surface sediments in the region. Opal content in the surface

353   sediments of the Southern Ocean increases from north to south, being the dominant

354   component south of the APF. In contrast, $CaCO_3$ is dominant north of the SAF and

355   decreases southward (Honjo et al., 2000).

356   Total mass and POC fluxes provided the strongest correlation at both sediment traps

357   (Table 2). As $BSiO_2$ dominated the mass fluxes throughout the sampling period,

358   changes in the $BSiO_2$ flux directly affected POC fluxes, suggesting that diatom valve

359   sedimentation plays an important role in controlling the organic carbon export to depth

360   at the AZ site. On the other hand, the small $CaCO_3$ fluxes and lower correlation values

361   with POC at both sediment traps suggest that $CaCO_3$ had a lesser influence on the POC

362   export. However, as the carrying capacity of POC per $CaCO_3$ unit could not be

363   quantified, the role of $CaCO_3$ in controlling the transfer of organic carbon to depth

364   remains unknown.

365

366   **4.3 Seasonal trend of diatom fluxes and species composition**

367   The annual diatom fluxes registered by the 2000 m sediment trap (Table 1) fall within

368   the range of those estimated by Fischer et al. (2002) in the AZ of the eastern Atlantic

369   (20×10^6 valves m^{-2} d^{-1}) and those reported by Grigorov et al. (2014) in the Ross Sea

370   Gyre (93×10^6 valves m^{-2} day^{-1}). The diatom fluxes recorded at site 61°S are therefore

comparable in magnitude to previously reported diatom data sets of the AZ in the Southern Ocean.

Although several factors, such as grazing, dissolution and lateral advection, can influence diatom flux (Boltovskoy et al. 1993), the similar seasonal patterns, with a two month offset between primary productivity and diatom flux variations (Figs. 2 and 5a) suggest that the primary signal of the phytoplankton bloom in the overlying water masses is registered by the traps. About two-thirds of the annual diatom export fluxes at each trap depth were registered during January and February (Fig. 5). A markedly seasonal pattern is characteristic of high latitude systems (e.g. Wefer et al., 1988; Dunbar et al., 1998; Honjo et al., 2000; Fischer et al., 2002; Pilskaln et al., 2004; Romero and Armand, 2010) and illustrates the opportunistic character (r selection) of the dominant species during the summer bloom. As a consequence of this rapid diatom biomass increase, silica in the AZ-S is often stripped out the mixed layer by mid-summer (Trull et al., 2001c).

The temporal variations in the composition of diatom assemblages mirrored the changes of the hydrographic conditions in the AZ-S, south of Tasmania. Overall, the major diatom taxa recorded at our mooring site are typical of living and fossil assemblages representing open ocean waters of the Antarctic Zone (Romero and Armand, 2010; Crosta et al., 2005, respectively).

The seasonal diatom flux was mainly driven by changes in the flux of the large, heavily-silicified and bloom-forming *F. kerguelensis*, a prominent member of the diatom assemblages in the iron-limited Southern Ocean waters (Smetacek, 1999; Abelmann et al., 2006). Large abundances of *F. kerguelensis* in phytoplankton blooms have also been previously reported in our study area during the SOIREE experiment (Gall et al., 2001; Trull and Armand, 2001), in the AZ of the south-west Atlantic (Hart, 1934) and in the

vicinity of open-ocean fronts in the Atlantic and Pacific sectors (Bathmann et al., 1997; Laubscher et al., 1993; Grigorov et al., 2014). The relative contribution of *F. kerguelensis* at both 61 S traps (68-80%; Table 1) is consistent with its distribution in the Southern Ocean surface sediments where its maximum abundances (70-83%) are found between the Polar Front and the maximum summer sea-ice edge (Crosta et al., 2005). Fischer et al. (2002) and Grigorov et al. (2014) reported lower relative abundance and fluxes of this species in sediment traps in the AZ of the Atlantic sector (29%; 6 x 10^6 valves m^{-2} d^{-1}) and in the Ross Sea Gyre (22%; 20 x 10^6 valves m^{-2} d^{-1}), respectively. However, these sites were under the influence of seasonal ice, where sea-ice affiliated taxa such as smaller *Fragilariopsis* species and *Chacetoceros* spp., are known to often dominate the diatom assemblages (Armand et al., 2005).

At the onset of the summer particle "bloom", H´ rises significantly due to the burst of reproduction and sedimentation of most of the diatom taxa (Fig. 5a). The small and rapidly dividing diatoms *Chaetoceros* group, *Fragilariopsis pseudonana*, *Fragilariopsis rhombica*, *Fragilariopsis separanda* and *Pseudo-nitzschia* spp., together with the cool open ocean species *Thalassiosira gracilis,* are major contributors to the bulk of the spring-summer maximum (Fig. 5). The majority of these diatoms correspond to the Group 1 defined by Quéguiner (2013), consisting of slightly silicified and fast-growing species that undergo rapid species succession during productive periods. The biomass accumulation of such diatoms is thought to be controlled principally by nutrient availability rather than grazing pressure. This concept agrees well with the observations of Zeldis (2001) who reported low grazing impact over the bloom development during the SOIREE experiment. At the end of their growth season, these bloom-forming species are considered to undergo mass mortality resulting in the formation of aggregates that rapidly sink from the euphotic zone (Assmy et al., 2013).

17

421 The AZ-S site is remote from the direct influence of sea-ice in summer (Massom et al.,

422 2013; Fig. 1b), which makes the occurrence of the sea-ice affiliated diatoms

423 *Fragilariopsis cylindrus* and *Fragilariopsis curta* during January (Fig. 5b) puzzling.

424 The distribution of *F. cylindrus* in the modern Southern Ocean is constrained to the

425 north by the maximum summer sea ice edge (Semina, 2003; Armand et al., 2005; Esper

426 et al. 2010), whereas *F. cylindrus* appears limited by the maximum extension of sea ice

427 during winter (Armand et al., 2005; Esper et al., 2010). Likely explanations for the

428 presence of these species at site 61°S are either (i) the occurrence of an iceberg in the

429 vicinity of our study area or (ii) the advection of a transient bloom produced in a region

430 under the influence of sea ice. Rich sea-ice affiliated diatom communities have been

431 found in association with free-drifting icebergs (e.g. Smith et al., 2011), however this

432 explanation is unlikely since our site is remote from any known iceberg pathway

433 (Gladstone et al., 2001). Taking into account a time lag of about two months between

434 peak production and particle export, a healthy and neutrally buoyant bloom could cover

435 a much larger distance than that estimated for a sinking particle (detailed in 4.5). Sea-ice

436 coverage west of ~90°E can reach latitudes well above 61°S (Massom et al., 2013; Fig.

437 1b). We hypothesize that the pulses of *F. curta* and *F. cylindrus* could correspond to the

438 sedimentation of a diatom bloom that was either advected from an area upstream the

439 ACC under the influence of seasonal sea ice or transported northward by Antarctic

440 Surface Water currents (AASW) produced by the seasonal retreat of the sea ice, south

441 of our study.

442 Enhanced fluxes of the large and thick-walled *F. kerguelensis* persisted for a longer

443 period (until April) than those of Group 1 (sensu Quéguiner, 2013) most likely

444 contributing to the progressive reduction of silicic acid concentrations in the mixed

445 layer throughout the summer. A similar pattern was reported by Assmy et al. (2013)

both inside and outside the iron-fertilized bloom during the European Iron Fertilization Experiment (EIFEX). *Fragilariopsis kerguelensis* is considered a "sinking-silica species" (Assmy et al., 2013) largely responsible for the decoupling of silicon and carbon cycles in the iron-limited ACC.

At the end of the diatom export maximum (i.e. February-March), *Thalassiothrix antarctica* contributed more significantly to the flux via increased abundances (Fig. 5b). This species is a large, slow-growing diatom distributed within discrete layers of the water column (Kemp et al., 2000). Such diatoms are considered k-strategists (Kemp and Villareal, 2013) and fall within Group 2 defined by Quéguiner (2013). High abundances of *Thalassiothrix antarctica* have been reported within and south of the APF (Laubscher et al., 1995; Bracher et al., 1999) and associated to a subsurface chlorophyll maximum in the PFZ south of Tasmania (Kopczynska et al., 2001; Parslow et al., 2001; Gomi et al., 2010) and in Prydz Bay (Quilty et al., 1985). We suspect that *Thalassiothrix antarctica* develops in parallel to Group 1 diatoms, as a result of them inhabiting the pycnocline discontinuity, exploiting deep nutrients and undergoing low rates of primary productivity under low-light conditions (Kemp et al., 2000, 2006; Quéguiner, 2013). The abrupt drop of the photosynthetically active radiation levels to less than half their peak values from February to March (Fig. 2a) and/or the occurrence of a vertical mixing event may have produced both light and/or nutrient limitation leading to the rapid flocculation and sinking of *T. antarctica* during the summer-autumn transition.

Post-March diatom export decreases significantly (Fig. 5a) due to the reduction to lowest levels of light and the concomitant intensification of mixing of the water column (Fig. 2a,b). The "post-bloom" diatom assemblage is characterized by low diversity values (Fig. 5a) mainly due to the high relative abundance of *F. kerguelensis* (up to 96% in September). The remaining assemblage is subsequently composed of large and

471 heavily silicified centrics such as *Thalassiosira lentiginosa, Azpeitia tabularis* and

472 *Thalassiosira oliveriana.* These are typical open ocean diatoms (Crosta et al., 2005;

473 Romero et al., 2005) with presumed lower nutrient requirements than the summer

474 bloom-forming species.

475

476 **4.4 Transfer to depth**

477 Our results suggest that a fast and relatively undisturbed downward transport of

478 particles occurred between 2000 and 3700 m (Fig. 3 and 4). The similar BSi and POC

479 content in both traps (Table 1) indicates that little silica dissolution and remineralization

480 occurred between 2000 and 3700 m. Such a result is consistent with previous sediment

481 trap studies that reported minimal alteration of the silica and organic carbon fluxes

482 below the mesopelagic-bathypelagic boundary (~2000 m) (Takahashi, 1986; Honjo et

483 al., 2009). However, the high Si/C at both depth levels also implies that organic matter

484 is recycled faster than opal before reaching the traps, and this must occur at mesopelagic

485 depths. We interpret this as the remineralization of the settling material by the microbial

486 community and by the zooplankton that preferentially feed on organic matter (Honjo,

487 2009). High Si/C ratios are characteristic of the iron-limited systems of the Southern

488 Ocean where large and highly silicified species (e.g. *Fragilariopsis kerguelensis*)

489 dominate the diatom assemblages. In this regard, the average POC content (1.4%) of

490 our samples at 2000 m is very low, and the average BSi/POC molar ratio for the entire

491 collection period was less than 0.1 for both traps, in comparison to an average of ~1 for

492 a compilation of deep Southern Ocean traps (Honjo et al., 2008) and a median of ~2 for

493 a global compilation (Lampitt and Antia, 1998). This makes it clear that the trap

494 samples have experienced very strong losses of organic carbon, consistent with previous

495   studies suggesting that Southern Ocean waters south of the Polar Front can be described

496   as low carbon export regimes (Lam and Bishop, 2007).

497   The sinking velocities of the major diatom taxa during the "particle bloom" indicate

498   rapid sedimentation of the diatom assemblages between the upper and lower traps (210

499   m d^{-1}). These settling speeds are very similar to those estimated by Honjo et al. (2000)

500   in the AZ of the Pacific Sector and are equal, or greater than, those observed in high

501   productivity areas at lower latitudes (Honjo, 1996). In contrast, based on the time delay

502   between samples with similar silicon isotopic signatures at different depths at site 61 S,

503   Closet et al. (unpublished results) estimated the settling velocities outside the

504   production period to be 120 m d^{-1} or less. These observations suggests that sinking rates

505   of diatom valves at site 61 S are related to flux size, perhaps because higher fluxes lead

506   to the formation of fast-sinking aggregates (e.g. Alldredge and Gotschalkt, 1989). This

507   concept is consistent with the observations of Grigorov et al. (2014) on sediment trap

508   material from the Pacific Sector of the Southern Ocean who reported abundant diatom

509   aggregates at times of peak flux and mainly individual cells and small chains outside the

510   production period. Moreover, the formation of aggregates would also explain the

511   enhanced POC export (Table 1) in association with high fluxes of Group 1 diatoms

512   during the production period (Assmy et al., 2013).

513   The pulse of *Thalassiothrix antarctica* in early March at both depths coincides with an

514   upturn of the POC fluxes (Table 1). *Thalassiothrix antarctica* cells are about 60 times

515   larger (in estimated biovolume) than *F. kerguelensis* (Cornet-Barthaux et al., 2007), and

516   therefore, have the potential to contribute significantly to the annual organic carbon

517   export even at background concentrations (Goldman 1993; Goldman and McGillicuddy,

518   2003; Quéguiner et al., 2013).

519   During winter, the lower sinking rates and high area/volume ratios of single diatom

520   cells may facilitate the recycling of the valves and remineralization of organic matter in

521   the upper water column. The enrichment of dissolution-resistant diatoms (e.g.

522   *Fragilariopsis kerguelensis*, *Thalassiosira oliveriana*, *Azpeitia tabularis*) during the

523   winter months observed in our traps could, therefore, be partially related to enhanced,

524   selective dissolution of more lightly silicified species (e.g. *Pseudo-nitzschia* spp.,

525   *Fragilariopsis pseudonana*, *Chaetoceros* spp.).

526   With regard to the comparison of the annual diatom assemblage between traps, their

527   highly similar abundance proportions, as revealed by the low squared chord distance

528   score, indicate that both traps registered diatom assemblages from the same source.

529   Moreover, the latter results further support the idea that silica BSi dissolution below

530   2000 m is minimal at the AZ-S site.

531

532   **CONCLUSIONS**

533   The main objective of our study was to document the variability in the magnitude,

534   timing and composition of particle and diatom export fluxes to the deep sea in the

535   southern Antarctic Zone (AZ-S) within the Australian sector of the Southern Ocean. To

536   examine this issue, we studied the year-round dynamics of particle flux from November

537   2001 through September 2002. The overall fluxes of biogenic particles to the mid- and

538   deep water column in the AZ-S were markedly seasonal with peak fluxes occurring

539   during the austral summer and very low export during winter. This seasonal pattern is

540   mediated by algal productivity. Comparison of satellite and particle flux data suggests a

541   delay of about two months between peak production and onset of particle export. The

542   biogenic opal fraction largely dominates the export throughout the year, and is mainly

543   delivered by diatoms. Carbonate and organic carbon are secondary components.

544   Diatom seasonal fluxes followed the seasonality of the biogeochemical particle fluxes at

545   both depths and their magnitude (67-76 x 10^6 valves m^{-2} day^{-1}) is similar to previously

546   published data recorded in the AZ of other sectors of the Southern Ocean. The diatom

547   assemblages recovered at our mooring site are typical of the open ocean waters of the

548   Antarctic Zone (Crosta et al., 2005) and their seasonal succession agrees well with the

549   conceptual scheme proposed by Quéguiner (2013) for the POOZ (Permanently Open

550   Ocean Zone) and the PFZ (Polar Frontal Zone). *Fragilariopsis kerguelensis* is, by far,

551   the most dominant diatom species in the sediment trap samples. The occurrence of the

552   sea-ice affiliated species *F. cylindrus* and *F. curta* may correspond to the sedimentation

553   of a diatom bloom advected from an area under the influence of sea ice upstream the

554   ACC. The sedimentation pulse of the deep-dwelling species *Thalassiothrix antarctica*

555   during the February-March transition appears to have been triggered by an abrupt drop

556   of the light levels and/or a vertical mixing event.

557   Finally, the good correlation between the total mass fluxes at both sediment traps and

558   their similar diatom species composition suggests fast and undisturbed settling of

559   particles through the deep water column at the AZ-S site.

560

578

579 **FIGURE CAPTIONS**

580 **Figure 1. a.** Location of the sediment trap mooring line in the Antarctic Zone of the

581 Australian sector of the Southern Ocean. Fronts (STF - Subtropical Front, SAF -

582 Subantarctic Front, PF - Polar Front, SB - Southern Boundary), regions (STZ –

583 Subtropical Zone, SAZ – Subantarctic Zone, PFZ – Polar Front Zone, ACC – Antarctic

584 Zone and SACCZ - Zone south of the ACC) and maximum extension of winter sea ice

585 (Max WSI) are shown. Triangle represents the position of 61°S mooring during the

586 experiment (Nov. 2001 – Sep. 2002). **b.** Mean sea ice season duration map for the East

587 Antarctic sector (1979/80-2009/10), with contours for 100, 200 and 300 days marked

588 (modified from Massom et al., 2013). **c.** Schematic diagram of the Australian sector of

589 the Southern Ocean depicting the bathymetry, main water masses and mooring

590 configuration. SAMW – Subantarctic Mode Water, AAIW – Antarctic Intermediate

591 Water, UCDW – Upper Circumpolar Deep Water, LCDW – Lower Circumpolar Deep

592 Water and AABW – Antarctic Bottom Water. Figure is adapted from Bostock et al.

593 (2013).

24

594

Figure 2: (**a**) Monthly mean chlorophyll-*a* concentration (mg m^{-3}), sea surface temperature (SST) (°C) and photosynthetically active radiation (Einstein m^{-2} d^{-1}) for the period November 2001 to September 2002. No data was available from April to August in 2001 and 2002. (**b**) Seasonal variation in the vertical structure of temperature (°C) at the 61°S site.

600

Figure 3. Temporal variability of the total mass and major biogenic fluxes for <1 mm fraction at 2000 and 3700 m water depth from November 2001 through to November 2002 at the 61°S site.

604

Figure 4. Correlation between (a) mass flux (mg m^{-2} day^{-1}) at 2000 and 3700 m, and (b) mass flux (mg m^{-2} day^{-1}) and diatom valve flux (10^6 m^{-2} day^{-1}) at 2000 and 3700 m.

607

Figure 5. Seasonal variation of (a) total diatom flux and Shannon's diversity index (H´) and (b) flux and relative abundance of the main diatom species at 2000 and 3700 m sediment traps. The arrows indicate the associated peaks of valve flux at both depths used to calculate the sinking velocities.

612

Figure 6: SEM photos of some of the most relevant diatom taxa collected by the sediment traps at site 61°S. (a) *Azpeitia tabularis*. (b) *Chaetoceros atlanticus* (resting stage). (c) *Fragilariopsis curta*. (d) *Fragilariopsis cylindrus*. (e) *Fragilariopsis kerguelensis*. (f) *Fragilariopsis pseudonana*. (g) *Fragilariopsis rhombica*. (h) *Fragilariopsis separanda*. (i) *Pseudo-nitzschia* spp. (j) *Thalassiosira gracilis* var.

25

618 *gracilis*. (k) *Thalassiosira lentiginosa*. (l) *Thalassiothrix antarctica*. Scale bars: d, f = 1

619 μm; h, i = 2 μm; c, e, j = 5 μm; a, b, g, k, l = 10 μm.

620

621 **Table 1:** Daily export fluxes of total mass flux, biogenic silica ($BSiO_2$), calcium

622 carbonate ($CaCO_3$), particulate organic carbon (POC) and diatom valves registered at

623 the 61°S site from November 2001 through October 2002. Mass fluxes listed as zero

624 were too small to measure (<1 mg). *Average diatom fluxes for the 2000 and 3700 m

625 traps have been estimated for different sampling intervals (309 and 172 days,

626 respectively).

627

628 **Table 2:** Correlation matrix (R^2) for the total mass and bulk compound fluxes at both

629 sediment traps.

630

631 **Table 3:** Integrated fractional abundances of the diatom taxa found at the 2000 and

632 3700 m sediment traps at station 61°S.

633

634 **REFERENCES**

635 Abelmann, A., Gersonde, R. (1991) Biosiliceous particle flux in the Southern Ocean,

636 *Mar. Chem.*, **35**, 503—536.

637

638 Abelmann, A., Gersonde, R., Cortese, G., *et al.* (2006) Extensive phytoplankton blooms

639 in the Atlantic Sector of the glacial Southern Ocean, *Paleoceanography*, **21**, PA1013

640

641 Acker, J.G. and Leptoukh, G. (2007) Online analysis enhances use of NASA Earth

642 science data. *Eos, Transactions*. AGU, **88**, 14–17.

643

644 Alldredge, A.L., Gotschalkt, C.C. (1989) Direct observations of the mass flocculation of

645 diatom blooms: characteristics, settling velocities and formation of diatom aggregates.

646 *Deep-Sea Res. (1 Oceanogr. Res. Pap.)*, **36** (2), 159–17

647

648 Arrigo, K.R., Robinson, D.H., Worthen, D.L., *et al.* (1999) Phytoplankton community

649 structure and the drawdown of nutrients and CO_2 in the Southern Ocean. *Science* **283**,

650 365–367.

651

652 Armand, L.K., Crosta, X., Romero, O.E. *et al.* (2005) The biogeography of major diatom

653 taxa in Southern Ocean surface sediments: 1. Sea ice related species. *Paleogeogr.,*

654 *Palaeoclimatol., Palaeoecol.,* **223**, 93–126.

655

656 Armand, L.K., Leventer, A. (2010) Palaeo sea ice distribution and reconstruction derived from the

657 geological record. In *Sea Ice,* (Eds. D. N. Thomas & G.S. Dieckmann, G.S.), pp. 469-530,

658 Wiley-Blackwell Publishing Ltd, Oxford.

659

660 Assmy, P., Smetacek, V., Montresor, M. (2013) Thick–shelled, grazer–protected diatoms

661 decouple ocean carbon and silicon cycles in the iron–limited Antarctic Circumpolar

662 Current. *PNAS* **110** (51) 20633–20638.

663

664 Baker, E.T., Milburn, H.B., Tennant, D.A. (1988) Field assessment of sediment trap

665 efficiency under varying flow conditions. *J. Mar. Res.* **46**, 573–592.

666

667 Bathmann, U., Fischer, G., Müller, P.J. *et al.* (1991) Short–term variations in particulate

668 matter sedimentation off Kapp Norvegia, Weddell Sea, Antarctica: relation to water

669   mass advection, ice cover, plankton biomass and feeding activity. *Polar Biol.* **11**, 185–

670   195.

671

672 Boltovskoy, D., Alder, V.A., Abelmann, A. (1993) Annual flux of Radiolaria and other

673   shelled plankters in the eastern equatorial Atlantic at 853 m: seasonal variations and

674   polycystine species-specific responses. *Deep-Sea Res. (1 Oceanogr. Res. Pap.)*, **40**(9),

675   1863–1895.

676

677 Bostock, H.C., Barrows, T.T., Carter, L. et al. (2013) A review of the Australian–New

678   Zealand sector of the Southern Ocean over the last 30 ka (Aus-INTIMATE project).

679   *Quat. Sci. Rev.* **74**, 35–57.

680

681 Boyd, P., Watson, J., Law, C.S. *et al.* (2000) Phytoplankton bloom upon mesoscale iron

682   fertilisation of polar Southern Ocean waters. *Nature* **407**, 695–702.

683

684 Bracher, A.U., Kroon, B.M.A., Lucas, M.I. (1999) Primary production, physiological

685   state and composition of phytoplankton in the Atlantic Sector of the Southern Ocean.

686   *Mar. Ecol. Pro. Ser.* **190**, 1–16.

687

688 Bray, S., Trull, T.W., Manganini, S. (2000) SAZ Project Moored Sediment Traps: Results

689   of the 1997–1998 Deployments, 128 pp, Antarct. Coop. Res. Cent., Hobart, Tasmania,

690   Australia.

691

692 Buesseler, K.O., L. Ball, J. Andrews, *et al.*, (2001) Upper ocean export of particulate

693   organic carbon and biogenic silica in the Southern Ocean along 170°W. *Deep-Sea Res.*

694   *(2 Top. Stud. Oceanogr.)* **48** (19–20), 4275–4297.

695

696   Coale, K.H., Johnson, K.S., Chavez, F.P., *et al.* (2004) Southern Ocean iron enrichment

697   experiment: Carbon cycling in high- and low-Si waters. *Science* **304** (5669), 408–414.

698

699   Comiso, J.C., Zwally, H.J. (1984) Concentration gradients and growth/decay

700   characteristics of the seasonal sea ice cover. *J. Geophys. Res*. **89**, 8081–8103.

701

702   Copin-Montegut, C., Copin-Montegut, G. (1983) Stoichiometry of carbon, nitrogen, and

703   phosphorus in marine particulate matter. *Deep-Sea Res. (1 Oceanogr. Res. Pap.)*, **30** (1),

704   31–46.

705

706   Cornet-Barthaux, V., Armand, L.K., Quéguiner, B. (2007) Biovolume and biomass

707   measurements of key Southern Ocean diatoms. *Aquat. Microb. Ecol.* **48** (3), 295–308.

708

709   Crosta, X., Romero, O., Armand, L.K., *et al.* (2005) The biogeography of major diatom

710   taxa in Southern Ocean sediments: 2. Open ocean related species. *Palaeogeogr.,*

711   *Palaeoclimatol., Palaeoecol.*, **223**, 66–92.

712

713   De Baar, H.J.W., de Jong, J.T.M., Bakker, D.C.E. *et al.* (1995) Importance of iron for

714   phytoplankton blooms and carbon dioxide drawdown in the Southern Ocean. *Nature*

715   **373**, 412–415.

716

717 Dunbar, R.B., Leventer, A.R. and Mucciarone, D.A. (1998) Water column sediment

718 fluxes in the Ross Sea, Antarctica: atmospheric and sea ice forcing. *J. Geophys. Res.*

719 **103** (30) 741–59

720

721 Esper, O., Gersonde, R., Kadagies, N. (2010). Diatom distribution in southeastern Pacific

722 surface sediments and their relationship to modern environmental variables.

723 *Palaeogeogr., Palaeoclimatol., Palaeoecol.*, 287, 1–27.

724

725 Fischer, G., Fütterer, D., Gersonde, R., *et al.* (1988) Seasonal variability of particle flux in

726 the Weddell Sea and its relation to ice cover. *Nature*, **335**, 426–8.

727

728 Fischer, G., Gersonde, R., Wefer, G. (2002) Organic carbon, biogenic silica and diatom

729 fluxes in the marginal winter sea-ice zone and in the Polar Front Region: interannual

730 variations and differences in composition. *Deep-Sea Res. (2 Top. Stud. Oceanogr.)*, **47**,

731 1721–1745.

732

733 Fitzwater, S.E. Johnson, K.S., Gordon, *et al.* (2000) Trace metal concentrations in the

734 Ross Sea and their relationship with nutrients and phytoplankton growth. *Deep-Sea Res.*

735 *(2 Top. Stud. Oceanogr.)*, **47**, 3159–3179.

736

737 Flores, J.A., Sierro, F.J. (1997) A revised technique for the calculation of calcareous

738 nannofossil accumulation rates. *Micropal.*, **43**, 321–324.

739

740 Gall, M.P., Boyd, P.W., Hall, J., *et al.* (2001) Phytoplankton processes. Part 1:

741 Community structure during the Southern Ocean Iron Release Experiment (SOIREE)

742   *Deep-Sea Res. (1 Oceanogr. Res. Pap.)*, **48**, 2551–2570.

743

744   Gardner, W.D. (1980) Sediment trap dynamics and calibration: a laboratory evaluation. *J.*

745   *Mar. Res.*, **38**, 17–39.

746

747   Gardner, W.D. (1985). The effect of tilt on sediment trap efficiency. *Deep-Sea Res. (1*

748   *Oceanogr. Res. Pap.)* **32**, 349–361.

749

750   Gladstone, R.M., Bigg, G.R., Nicholls, K.W. (2001) Iceberg trajectory modelling and

751   meltwater injection in the Southern Ocean. *J. Geophys Res.*, **106** (9), 19903–19915.

752

753   Goldman, J.C. (1993) Potential role of large oceanic diatoms in new primary production.

754   *Deep-Sea Res. (1 Oceanogr. Res. Pap.)* **40** (1), 159–168.

755

756   Goldman, J.C., McGillicuddy, D.J. (2003) Effect of large marine diatoms growing at

757   low light on episodic new production. *Limnol. Oceanogra.*, **48** (3), 1176–1182.

758

759   Gomi, Y., Fukuchi, M., Taniguchi, A. (2010) Diatom assemblages at subsurface

760   chlorophyll maximum layer in the eastern Indian sector of the Southern Ocean in

761   summer. *J. Plank. Res.* **32** (7), 1039–1050.

762

763   Grigorov, I., Rigual-Hernandez, A.S., Honjo, S., *et al.* (2014) Settling fluxes of diatom

764   frustules to the interior of the Antarctic Circumpolar Current along 170°W. *Deep-Sea*

765   *Res. (1 Oceanogr. Res. Pap.)*, **93**, 1-13.

766

767 Hallegraeff, G.M. (1986) Taxonomy and morphology of the marine plankton diatoms

768   *Thalassionema* and *Thalassiothrix*. Diatom Research, **1**, 57-80.

769

770 Hart, T. (1934) On the phytoplankton of the South-West Atlantic and the Bellinghausen

771   Sea, 1929–31. *Discovery Reports*, **8**, 1–268.

772

773 Heussner, S., Durrieu De Madron, X., Calafat, A. *et al.* (2006) Spatial and temporal

774   variability of downward particle fluxes on a continental slope: Lessons from an 8-yr

775   experiment in the Gulf of Lions (NW Mediterranean) *Mar. Geol.*, **234**, 63–92.

776

777 Honjo, S. (1996) Fluxes of particles to the interior of the open oceans, in Particle Flux in

778   the Ocean, edited by V. Ittekkot *et al.*, pp. 91–154, John Wiley, New York.

779

780 Honjo, S. (2009) Biological pump and particulate fluxes. In: Steele, J.H., Thorpe, S.A.,

781   Turekian, K.K. (Eds.) *Encyclopaedia of ocean sciences*. Academic Press, San Diego,

782   CA, 371–375

783

784 Honjo, S., Doherty, K.W. (1988) Large aperture time-series sediment traps; design

785   objectives, construction and application. *Deep-Sea Res.* **35**(1), 133–149

786

787 Honjo, S., Francois, R., Manganini, S., *et al.* (2000) Particle fluxes to the interior of the

788   Southern Ocean in the Western Pacific sector along 170 degrees W. *Deep-Sea Res. (2*

789   *Top. Stud. Oceanogr.)*, **47** (15–16), 3521–3548.

790

791 Honjo, S., Manganini, S.J., Krishfield, R.A. *et al.* (2008) Particulate organic carbon fluxes

792   to the ocean interior and factors controlling the biological pump: A synthesis of global

793   sediment trap programs since 1983. *Progr. Ocean.*, **76** (3), 217–285.

794

795 Honjo, S., Spencer, D.W., Gardner, W.D. (1992) A sediment trap intercomparison

796   experiment in the Panama Basin, 1979. *Deep-Sea Res. (1 Oceanogr. Res. Pap.)* **39**,

797   333–358.

798

799 Ichinomiya, M., Gomi, Y., Nakamachi, M., *et al.* (2008) Temporal variations in the

800   abundance and sinking flux of diatoms under fast ice in summer near Syowa Station,

801   East Antarctica. *Polar Science*, **2**, 33–40.

802

803 Ishikawa, A., Wasiyama, N., Tanimura, A., *et al.* (2001) Variation in the diatom

804   community under fast ice near Syowa Station, Antarctica, during the austral summer of

805   1997/98. *Polar Bioscience*, **14**, 10–23.

806

807 Johnson, K.S., Gordon, R.M. and Coale, K.H. (1997) What controls dissolved iron

808   concentrations in the world ocean?. *Mar. Chem.*, **57** (3–4), 137-161.

809

810 Kemp, A.E.S., Pike, J., Pearce, R.B. *et al.* (2000) The "Fall dump" a new perspective on

811   the role of a "shade flora" in the annual cycle of diatom production and export flux.

812   *Deep-Sea Res. (1 Oceanogr. Res. Pap.)*, **47**, 2129–2154.

813

814 Kemp, A.E.S., Pearce, R.B., Grigorov, I. (2006) Production of giant marine diatoms and

815   their export at oceanic frontal zones:implications for Si and C flux from stratified

816   oceans. *Global Biogeochem. Cycles* **20** (4), GB4S04.

817

818 Kemp, A.E.S., Villareal, T.A. (2013) High diatom production and export in stratified

819   waters – A potential negative feedback to global warming. *Progr. Ocean.*, **119** (0), 4–

820   23.

821

822 Kimura, N., Wakatsuchi, M. (2011) Large-scale processes governing the seasonal

823   variability of Antarctic sea-ice area. *Tellus* **63A**, 828–840.

824

825 Kopczynska, E.E., Dehairs, F., Elskens, M. *et al.* (2001) Phytoplankton and

826   microzooplankton variability between the Subtropical and Polar Fronts south of

827   Australia: Thriving under regenerative and new production in late summer. *J. Geophys.*

828   *Res.*, 106, 31597–31609.

829

830 Lam, P. J., Bishop, J.K.B. (2007) High biomass low export regimes in the southern ocean.

831   *Deep-Sea Res. (2 Top. Stud. Oceanogr.)*, **54** (5–7), 601–638

832

833 Lampitt, R.S., Antia, A.N. (1997) Particle flux in deep seas: regional characteristics and

834   temporal variability. *Deep-Sea Res. (1 Oceanogr. Res. Pap.)*, **44** (8): 1377–1403.

835

836 Laubscher, R.K., Perissinotto, R. and McQuaid, C.D. (1993) Phytoplankton production

837   and biomass at frontal zones in the Atlantic Sector of the Southern Ocean. *Polar Biol.*,

838   **13**, 471–481.

839

840 Leventer, A., Dunbar, R.B. (1987) Diatom flux in McMurdo Sound, Antarctica. *Mar.*

841   *Micropaleontol.*, **12**, 49–64.

842

843 Leventer, A., Dunbar, R.B., DeMaster, D.J. (1993) Diatom Evidence for Late Holocene

844   Climatic Events in Granite Harbor, Antarctica. *Paleoceanography* **8**, 373-386.

845

846 Leventer, A., Dunbar, R.B., (1996) Factors influencing the distribution of diatoms and

847   other algae in the Ross Sea. *J. Geophys. Res.*, **101**, 18489–500.

848

849 Locarnini, R.A., Mishonov, A.V. and Antonov, J.I. (2010) *World Ocean Atlas 2009*,

850   Volume 1: Temperature. Vol. 1, U.S. Government Printing Office, Washington, D.C.

851

852 Massom, R., Reid, P., Stammerjohn, S., *et al.* (2013) Change and Variability in East

853   Antarctic Sea Ice Seasonality, 1979/80–2009/10. *Plos one* **8** (5), e64756.

854

855 Martin, J.H., Fitzwater, S.E., Gordon, R. M. (1990) Iron deficiency limits phytoplankton

856   growth in Antarctic waters. *Global Biogeochem. Cycles* **4**, 5-12.

857

858 Matsumoto K., Sarmiento J.L. and Brzezinski M.A. (2002) Silicic acid leakage from the

859   Southern Ocean: A possible explanation for glacial atmospheric pCO2. *Global*

860   *Biogeochem. Cycles*, **16**, 1031.

861

862 Moore, J.K., Abbott, M.R. (2000) Phytoplankton chlorophyll distributions and primary

863   production in the Southern Ocean. *J. Geophys. Res.*, **105**, 28709–28722.

864

865 Nelson, D.M., Tréguer, P., Brzezinski, M.A., *et al.* (1995) Production and dissolution of

866 biogenic silica in the ocean: Revised global estimates, comparison with regional data

867 and relationship to biogenic sedimentation. Global Biogeochem. Cycles, 9, 359–372.

868

869 Orsi, A.H., Whitworth III, T., Nowlin Jr., W.D. (1995) On the meridional extent and

870 fronts of the Antarctic Circumpolar Current. *Deep-Sea Res. (1 Oceanogr. Res. Pap.)*,

871 **42**, 641–673.

872

873 Ortiz, J.D., Mix, A.C. (1997) Comparison of Imbrie-Kipp transfer function and modern

874 analog temperature estimates using sediment trap and core top foraminiferal faunas.

875 *Paleoceanography*, **12**, 175–190.

876

877 Parslow, J., Boyd, P., Rintoul, S.R. *et al.* (2001) A sub-surface chlorophyll maximum in

878 the Polar Frontal Zone south of Australia: seasonal evolution and implications for

879 phytoplankton-light-nutrient interactions. *J. Geophys. Res.*, **106**, 31543–31550.

880

881 Pilskaln, C.H., Manganini, S.J., Trull, T., *et al.* (2004) Geochemical particle fluxes in the

882 Southern Indian Ocean seasonal ice zone: Prydz Bay region, east Antarctica. *Deep-Sea*

883 *Res. (1 Oceanogr. Res. Pap.)*, **50**, 307–32.

884

885 Pondaven, P., Ragueneau, O., Tréguer, P., *et al.* (2000) Resolving the `opal paradox' in

886 the Southern Ocean. *Nature*, **405**, 168–172.

887

888 Popp, B.N., Trull, T., Kenig, F. *et al.* (1999) Controls on the carbon isotopic composition
889   of Southern Ocean phytoplankton. *Global Biogeochem. Cycles* **13** (4), 827–843.

890

891 Quéguiner, B. (2013) Iron fertilization and the structure of planktonic communities in
892   high nutrient regions of the Southern Ocean. *Deep-Sea Res. (1 Oceanogr. Res. Pap.)*I,
893   **90**, 43-54.

894

895 Quilty, P., Kerry, K.R., Marchant, H.J. (1985) A seasonally recurrent patch of Antarctic
896   planktonic diatoms. *Search (ANZAAS)*, **16**, 48.

897

898 Reynolds, R.W., Rayner, N.A., Smith, T.M. *et al.* (2002) An improved in situ and satellite
899   SST analysis for climate. *J. Climate*, **15**, 1609–1625.

900

901 Rintoul, S.R., Bullister, J.L. (1999) A late winter Hydrographic section from Tasmania to
902   Antarctica. *Deep-Sea Res. (1 Oceanogr. Res. Pap.)*, **46**, 1417–1454.

903

904 Rintoul, S.R., Sokolov, S. (2001) Baroclinic transport variability of the Antarctic
905   Circumpolar Current south of Australia (WOCE repeat section SR3). *J. Geophys. Res.*
906   **106**, 2795–2814.

907

908 Romero, O., Armand, L.K., Crosta, X. *et al.* (2005) The biogeography of major diatom
909   taxa in Southern Ocean sediments: 3. Tropical/Subtropical species. *Palaeogeogr.,*
910   *Palaeoclimatol., Palaeoecol.*, **223**, 49–65.

911

912 Romero, O.E., Fischer, G., Lange, C.B. *et al.*(2000) Siliceous phytoplankton of the

913   western equatorial Atlantic: sediment traps and surface sediments. *Deep-Sea Res. (2*

914   *Top. Stud. Oceanogr.)* **47**, 1939–1959.

915

916 Romero, O.E., Lange, C.B., Fischer, *et al.* (1999). Variability in export production

917   documented by downward fluxes and species composition of marine planktonic

918   diatoms: observations from the tropical and equatorial Atlantic. In: Fischer, G., Wefer,

919   G. (Eds.), The Use of Proxies in Paleoceanography, Examples from the South Atlantic.

920   Springer, Berlin, Heidelberg, pp. 365–392.

921

922 Romero, O., Thunell, R.C., Astor, Y., et al. (2009) Seasonal and interanual dynamics in

923   diatom production in the Cariaco Basin, Venezuela. *Deep-Sea Res. (1 Oceanogr. Res.*

924   *Pap.)*, **56**, 571–581.

925

926 Sakshaug, E., Holm-Hansen, O. (1984) Factors governing pelagic production in polar

927   oceans. In: Holm-Hansen, O., Bolis, L., Gilles, R. (Eds.), *Marine Phytoplankton and*

928   *Productivity. Lecture Notes on Coastal and Estuarine Studies*, vol. 8. Springer, Berlin,

929   pp. 1–18.

930

931 Sancetta, C., Calvert, S.E. (1988) The annual cycle of sedimentation in Saanich Inlet,

932   British Columbia: implications for the interpretation of diatom fossil assemblages. *Deep*

933   *Sea Res.* **35** (1), 71–90

934

935 Sarmiento, J.L.*,* T.M.C. Hughes*,* R.J. Stouffer *et al.* (1998) Simulated response of the

936   ocean carbon cycle to anthropogenic climate warming, *Nature,* **393***,* 245–249.

937

938 Schrader, H. J., Gersonde, R. (1978) Diatoms and silicofagellates. Micropaleontological

939   counting methods and techniques: an exercise on an eight metres section of the Lower

940   Pliocene of Capo Rosello, Sicily. *Utrecht Bull. Micropaleontol*. **17**, 129–176.

941

942 Semina, H.J. (2003) SEM-studied diatoms of different regions of the World Ocean.

943   Iconographia Diatomologica **10**, 1– 362.

944

945 Smetacek, V. (1985) Role of sinking in diatom life-history cycles: ecological,

946   evolutionary and geological significance. *Mar. Biol.* **84**, 239-251.

947

948 Smetacek, V. (1999). Diatoms and the ocean carbon cycle. *Protist*, **250**, 25– 32

949

950 Smetacek, V., Assmy, P., Henjes, J. (2004) The role of grazing in structuring Southern

951   Ocean pelagic ecosystems and biogeochemical cycles. *Antarctic Science*, **16**: 541–558.

952

953 Smith Jr., W.O., Nelson, D.M. (1986) Importance of ice edge phytoplankton production

954   in the Southern Ocean. *Bioscience* **36** (4), 251–257.

955

956 Smith Jr., K.L., Sherman, A.D., Shaw, T.J. *et al.* (2011) Carbon export associated with

957   free-drifting icebergs in the Southern Ocean. *Deep-Sea Res. (2 Top. Stud. Oceanogr.)*

958   **58**, (11–12), 1485–1496.

959

960 Sohrin, Y., Iwamoto, S., Matsui, M. *et al.* (2000) The distribution of Fe in the Australian

961   sector of the Southern Ocean. *Deep-Sea Res. (1 Oceanogr. Res. Pap.)*, **47,** 55–84.

962

963 Sokolov, S., Rintoul, S.R. (2002) Structure of southern ocean fronts at 140 E. *J. Mar.*

964 *Syst.* **37**, 151–184.

965

966 Sokolov, S., Rintoul, S.R. (2007) Multiple Jets of the Antarctic Circumpolar Current

967 South of Australia. *J. Physical Oceanogr.*, **37**, 1394–1412

968

969 Sokolov, S., Rintoul, S.R. (2009a) Circulation structure and distribution of the Antarctic

970 Circumpolar Current fronts: 1. Mean circumpolar paths. *J. Geophys. Res.* **114**, C11018.

971

972 Sokolov, S., Rintoul, S.R. (2009b) Circulation structure and distribution of the Antarctic

973 Circumpolar Current fronts: 2. Variability and relationship to sea surface height. J.

974 *Geophys. Res.* **114**, C11019.

975

976 Sullivan, C.W., McClain, C.R., Comiso, J.C., Smith, W.O. (1988) Phytoplankton standing

977 crops within an Antarctic ice edge assessed by satellite remote sensing. *J. Geophys. Res.*

978 **93**, 12487–12498.

979

980 Suzuki, H., Sasaki, H., Fukuchi, M. (2001) Short-term variability in the flux of rapidly

981 sinking particles in the Antarctic Marginal Ice Zone. *Polar Biol.* **24**, 697–705.

982

983 Takahashi, K. (1986) Seasonal fluxes of pelagic diatoms in the subarctic Pacific, 1982–

984 1983. Deep-Sea Res. **33**, 1225–51.

985

986 Taylor, F., Sjunneskog, C. (2002) Postglacial marine diatom record of the Palmer Deep,

987 Antarctic Peninsula (ODP Leg 178, Site 1098) 2. Diatom assemblages.

988 *Paleoceanography* **17**, PAL 2-1-PAL 2-12.

989

990 Tréguer, P. J., De La Rocha, C. L. (2013) The world ocean silica cycle. *Annual review of*

991 *marine science*, 5, 477-501.

992

993 Trull, T., Armand, L. (2001) Insights into Southern Ocean Carbon export from the δ 13 C

994 of particles and dissolved inorganic carbon during the SOIREE iron release experiment.

995 *Deep-Sea Res. (2 Top. Stud. Oceanogr.)*, **48**, 2655–2680.

996

997 Trull, T., SedwickF, P.N., Griffiths, F.B. et al. (2001a) Introduction to special section:

998 SAZ Project. *J. Geophys. Res.*, **106**, 31425–31429.

999

1000 Trull, T., Bray, S., Manganini, S., *et al.* (2001b) Moored sediment trap measurements of

1001 carbon export in the Subantarctic and Polar Frontal Zones of the Southern Ocean, south

1002 of Australia, *J. Geophys. Res.*, **106**, 31489–31510.

1003

1004 Trull, T., Rintoul, S. R., Hadfield, M., *et al.* (2001) Circulation and seasonal evolution of

1005 polar waters south of Australia: Implications for iron fertilization of the Southern

1006 Ocean, *Deep-Sea Res. (1 Oceanogr. Res. Pap.)*, **48**, 2439–2466

1007

1008 Varela, D.E., Pride, C.J., Brzezinski, M.A. (2004) Biological fractionation of silicon

1009 isotopes in Southern Ocean surface waters. Global Biogeochem. Cy., **18**, GB1047.

1010

1011 Wefer, G., Fischer, G., F. Utterer, D. *et al.* (1988) Seasonal particle flux in the Bransfield

1012 Strait, Antarctica. *Deep-Sea Res. (1 Oceanogr. Res. Pap.)* **35** (6), 891–898.

1013

1014 Yu, E.F., Francois, R., Bacon, M.P. *et al.* (2001) Trapping efficiency of bottom-tethered

1015 sediment traps estimated from the intercepted fluxes of ^{230}Th and ^{231}Pa *Deep-Sea Res.*

1016 *(1 Oceanogr. Res. Pap.)*, **48** (3) 865–889.

1017

1018 Zeldis, J. (2001) Mesozooplankton community composition, feeding, and export

1019 production during SOIREE. *Deep-Sea Res. (2 Top. Stud. Oceanogr.)*, 48, 2615–2634.

1020

61_2000	Sampling period	Length	Total Mass Flux	BSiO$_2$		CaCO$_3$		POC		POC/PN	Diatoms
Cup	mid point	days	mg m^{-2} d^{-1}	mg m^{-2} d^{-1}	%	mg m^{-2} d^{-1}	%	mg m^{-2} d^{-1}	%	molar ratio	10^6 valves m^{-2} d^{-1}
1	Nov. 30, 2001	8	48	26	54	14	30	0.7	1.5	6.6	-
2	Dec. 08, 2001	8	78	47	61	17	22	1.7	2.2	6.1	9
3	Dec. 16, 2001	8	326	198	61	62	19	6.9	2.1	5.4	82
4	Dec. 24, 2001	8	509	326	64	140	28	6.4	1.3	3.5	85
5	Jan. 01, 2002	8	1151	856	74	44	4	26.9	2.3	7.4	408
6	Jan. 09, 2002	8	1069	796	75	170	16	14.8	1.4	4.9	200
7	Jan. 17, 2002	8	656	478	73	60	9	11.3	1.7	6.1	159
8	Jan. 25, 2002	8	702	541	77	38	5	11.0	1.6	6.1	296
9	Feb. 02, 2002	8	666	520	78	39	6	12.0	1.8	6.5	184
10	Feb. 10, 2002	8	595	469	79	24	4	8.2	1.4	6.2	295
11	Feb. 18, 2002	8	534	425	80	20	4	6.2	1.2	6.5	149
12	Feb. 26, 2002	8	524	418	80	19	4	4.7	0.9	6.5	152
13	Mar. 06, 2002	8	586	471	80	15	3	6.9	1.2	7.2	120
14	Mar. 14, 2002	8	285	230	81	11	4	3.2	1.1	6.6	71
15	Mar. 22, 2002	8	290	253	87	7	3	3.2	1.1	6.8	66
16	Mar. 30, 2002	8	263	218	83	8	3	2.6	1.0	6.1	87
17	Apr. 08, 2002	10	264	220	83	7	3	2.2	0.8	6.4	97
18	May. 08, 2002	50	130	102	78	5	4	1.2	1.0	5.9	47
19	Jun. 29, 2002	54	65	52	79	2	4	0.7	1.0	6.6	10
20	Aug. 22, 2002	55	56	44	78	2	4	0.8	1.5	6.6	19
21	Sep. 29, 2002	20	42	34	81	2	4	0.5	1.3	7.2	6
Annualised values			**232**	**178**	**76**	**17**	**7.4**	**3.3**	**1.4**	**6.1**	**67**
Annual flux			**85 g m^{-2} y^{-1}**	**65 g m^{-2} y^{-1}**		**6 g m^{-2} y^{-1}**		**1.2 g m^{-2} y^{-1}**			**24 10^9 valves m^{-2} y^{-1}**

61_3700	Sampling period	Length	Total Mass Flux	BSiO$_2$		CaCO$_3$		POC		POC/PN	Diatoms
Cup	mid point	days	mg m^{-2} d^{-1}	mg m^{-2} d^{-1}	%	mg m^{-2} d^{-1}	%	mg m^{-2} d^{-1}	%	molar ratio	10^6 valves m^{-2} d^{-1}
1	Nov. 30, 2001	8	38	25	64	9	23	0.4	1.1	7.4	-
2	Dec. 08, 2001	8	31	17	54	9	28	0.4	1.2	6.4	-
3	Dec. 16, 2001	8	99	51	52	29	30	1.4	1.4	6.7	4
4	Dec. 24, 2001	8	231	148	64	59	26	1.4	0.6	2.6	12
5	Jan. 01, 2002	8	873	656	75	87	10	17.3	2.0	6.8	118
6	Jan. 09, 2002	8	1157	886	77	154	13	19.8	1.7	6.9	479
7	Jan. 17, 2002	8	828	611	74	166	20	9.4	1.1	4.6	354
8	Jan. 25, 2002	8	490	376	77	34	7	6.4	1.3	6.4	169
9	Feb. 02, 2002	8	491	384	78	32	6	6.5	1.3	6.1	385
10	Feb. 10, 2002	8	419	335	80	19	4	6.0	1.4	7.0	281
11	Feb. 18, 2002	8	584	475	81	36	6	6.2	1.1	6.2	254
12	Feb. 26, 2002	8	581	473	81	31	5	5.2	0.9	5.5	238
13	Mar. 06, 2002	8	849	737	87	23	3	7.6	0.9	6.5	326
14	Mar. 14, 2002	8	369	233	63	18	5	3.3	0.9	6.5	44
15	Mar. 22, 2002	8	218	174	80	8	4	2.6	1.2	7.3	32
16	Mar. 30, 2002	8	258	198	77	10	4	2.5	1.0	7.2	43
17	Apr. 08, 2002	10	257	202	79	9	3	2.3	0.9	6.9	32
18	May. 08, 2002	50	118	98	83	5	4	1.2	1.0	6.3	8
19	Jun. 29, 2002	54	0	0	83	0	4	0.0	1.0	6.3	-
20	Aug. 22, 2002	55	0	0	83	0	4	0.0	1.0	6.3	-
21	Sep. 29, 2002	20	0	0	83	0	4	0.0	1.0	6.3	-
Annualised values			**188**	**146**	**78**	**17**	**9**	**2.3**	**1.2**	**6.2**	**62**
Annual flux			**69 g m^{-2} y^{-1}**	**53 g m^{-2} y^{-1}**		**6 g m^{-2} y^{-1}**		**0.9 g m^{-2} y^{-1}**			**23 10^9 valves m^{-2} y^{-1}**

Table 1

2000 m	Total Mass Flux	$BSiO_2$	$CaCO_3$	POC
Total Mass Flux	-			
$BSiO_2$	0.99	-		
$CaCO_3$	0.37	0.30	-	
POC	0.86	0.83	0.24	-

3700 m	Total Mass Flux	$BSiO_2$	$CaCO_3$	POC
Total Mass Flux	-			
$BSiO_2$	0.99	-		
$CaCO_3$	0.61	0.54	-	
POC	0.87	0.83	0.63	-

Table 2

	2000m		3700 m
	Average 309 days	Average 172 days	Average 172 days
Actinocyclus spp.	0.01	0.01	0.03
Actinocyclus actinochilus (Ehrenberg) Simonsen	0.02	0.01	0.00
Asteromphalus hookeri Ehrenberg	0.17	0.20	0.48
A. hyalinus Karsten	0.16	0.26	0.29
A. parvulus Karsten	0.19	0.32	0.35
Asteromphalus spp.	0.01	0.01	0.01
Azpeitia tabularis (Grunow) Fryxell et Sims	0.68	0.57	0.74
Chaetoceros aequatorialis var. *antarcticus* Manguin	0.02	0.03	0.06
Ch. atlanticus Cleve	0.16	0.29	0.37
Ch. dichaeta Ehrenberg	0.11	0.19	0.16
Ch. peruvianus Brightwell	0.00	0.00	0.01
Chaetoceros sp. A	0.08	0.14	0.11
Chaetoceros sp. B	0.07	0.13	0.19
Chaetoceros spp.	0.15	0.27	0.32
Chaetoceros Hyalochaete resting spores	0.14	0.25	0.14
Corethron spp.	0.01	0.01	0.00
Dactyliosolen antarcticus Castracane			
Eucampia antarctica (Castracane) Mangin	0.13	0.14	0.20
Fragilariopsis curta (Van Heurck) Hustedt	0.57	1.00	1.11
F. cylindrus (Grunow) Krieger	0.16	0.29	0.10
F. kerguelensis (O'Meara) Hustedt	79.91	72.41	68.34
F. obliquecostata (van Heurck) Heiden	0.02	0.03	0.05
F. pseudonana (Hasle) Hasle	2.03	3.64	1.43
F. rhombica (O'Meara) Hustedt	0.93	1.58	2.13
F. ritscheri Hustedt	0.07	0.13	0.11
F. separanda Hustedt	2.10	2.85	2.03
F. cf. *sublineata* (Van Heurck) Heiden	0.03	0.04	0.03
Haslea trompii (Cleve) Simonsen	0.01	0.01	0.02
Navicula directa (Smith) Ralfs in Pritchard	0.33	0.58	1.06
N. sicula var. *bicuneata* (Castracane) Grunow	0.06	0.10	0.14
Pleurosigma directum Grunow in Van Heurck	0.02	0.03	0.03
Pseudo-nitzschia < 3 μm transapical axis	0.40	0.72	1.41
P-n. heimii Manguin	0.01	0.02	0.02
Pseudo-nitzschia spp.	0.11	0.19	0.08
Porosira pseudodenticulata (Hustedt) Jousé	0.02	0.03	0.03
Proboscia spp.	0.00	0.00	0.01
Rhizosolenia antennata (Ehrenberg) Brown f. *semispina* Sundström	0.00	0.00	0.02
Rhizosolenia bergonii Peragallo	0.00	0.00	0.02
Rhizosolenia sp. f. 1A (Armand et Zielinski)	0.01	0.01	0.02
Rhizosolenia spp.	0.09	0.07	0.02
Thalassionema nitzschioides f. *capitulata* (Castracane) Moreno-Ruiz	0.06	0.09	0.11
T. nitzschioides f. *lanceolata* (Grunow) Pergallo et Pergallo	0.05	0.02	0.02
Stellarima stellaris (Roper) Hasle et Sims	0.00	0.00	0.02
Thalassiosira gravida Cleve	0.03	0.05	0.11
T. gracilis var. *gracilis* (Karsten) Hustedt	3.65	6.08	7.41
T. gracilis var. *expecta* (Van Landingham) Frxyell et Hasle	0.42	0.65	1.30
T. lentiginosa (Janisch) Fryxell	4.97	4.63	6.77
T. maculata Fryxell et Johansen	0.05	0.02	0.02
T. oestrupii (Ostenfeld) Hasle	0.01	0.02	0.01
T. oliveriana (O'Meara) Makarova et Nikolaev	0.67	0.37	0.42
T. tumida (Janisch) Hasle	0.12	0.07	0.10
T. leptopus (Grunow ex Van Heurck) Hasle et G.Fryxell	0.01	0.01	0.54
T. lineata Jousé	0.11	0.14	0.36
Thalassiosira spp. < 20 μm	0.37	0.62	0.29
Thalassiosira spp. > 20 μm	0.04	0.05	0.00
Thalassiosira sp. A	0.18	0.22	0.01
Thalassiosira sp. B	0.02	0.03	0.08
Thalassiothrix antarctica Schimper ex Karsten	0.20	0.18	0.58
Tropidoneis group	0.04	0.05	0.12
Other centrics	0.07	0.07	0.02
Other pennates	0.01	0.01	0.01

Table 3

Figure 1
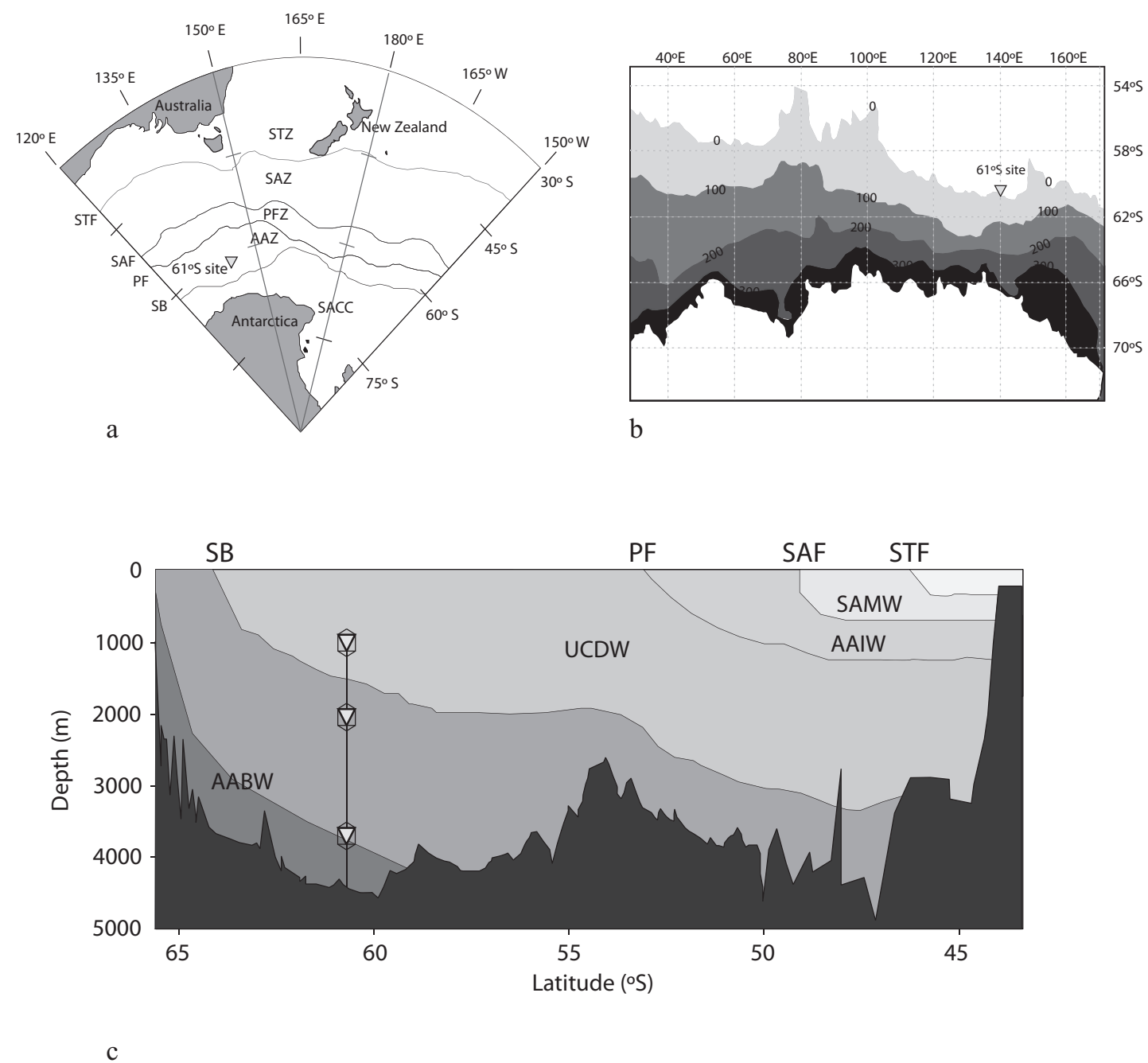
a

b

c
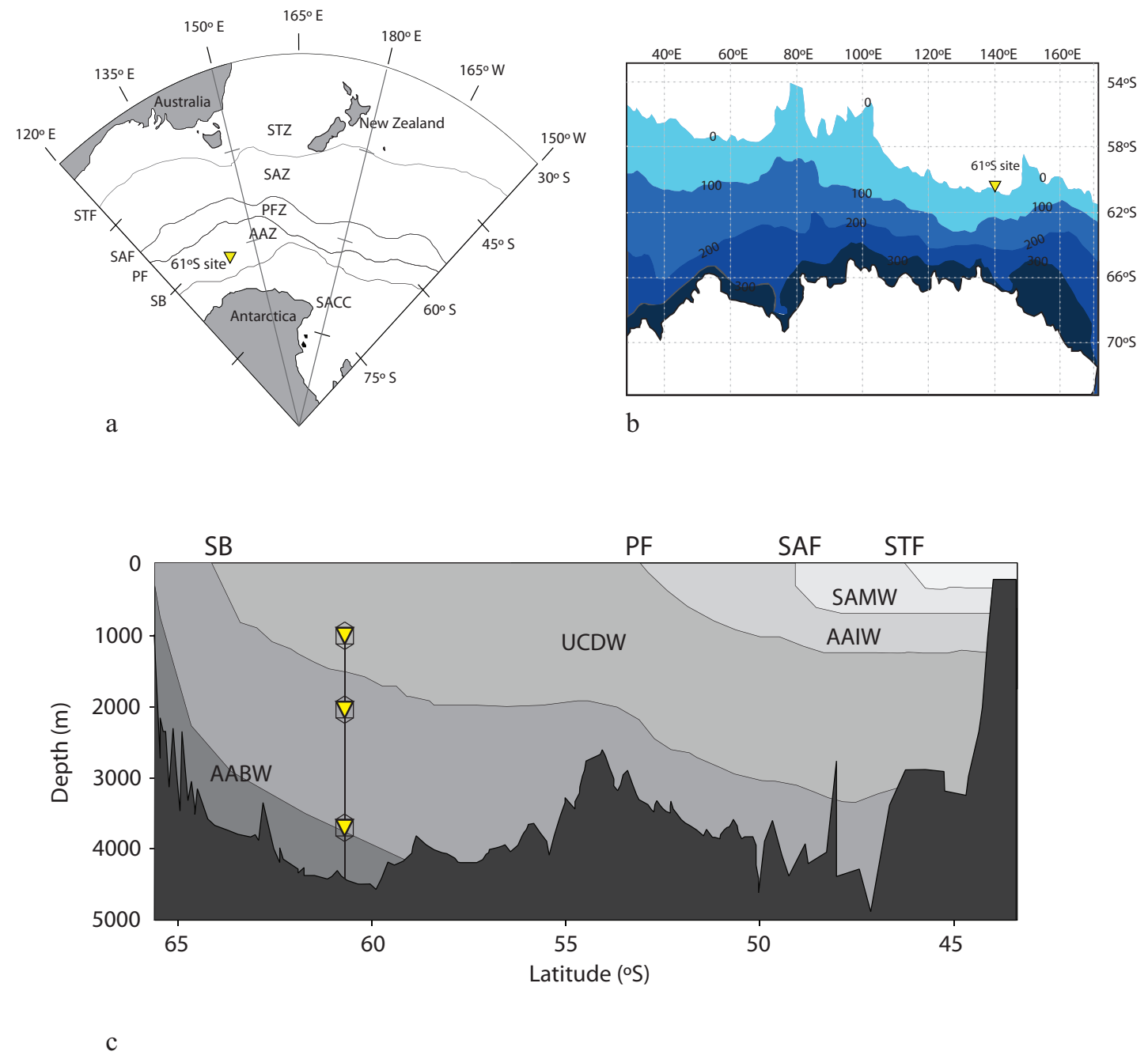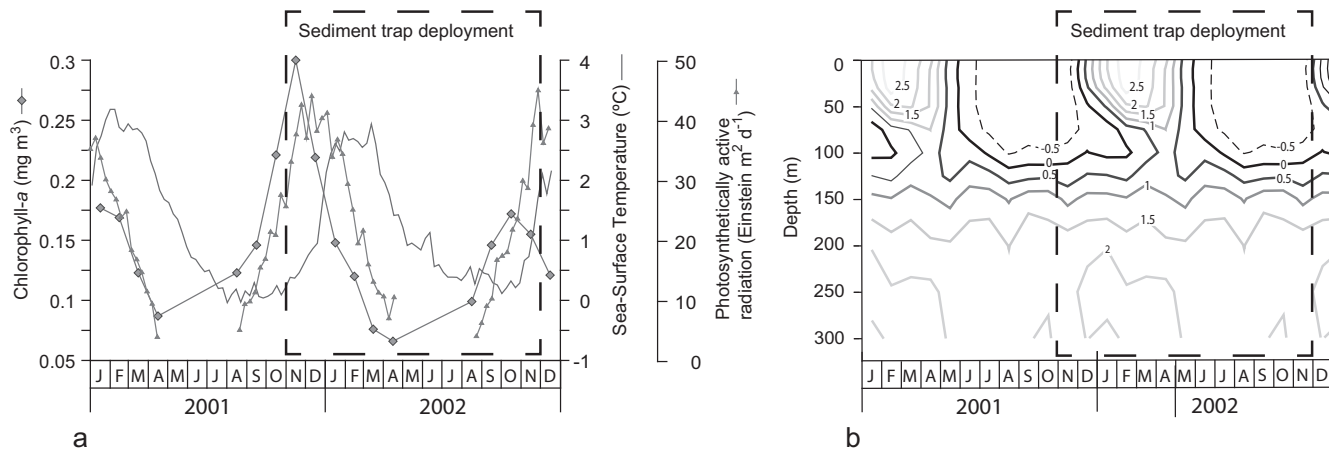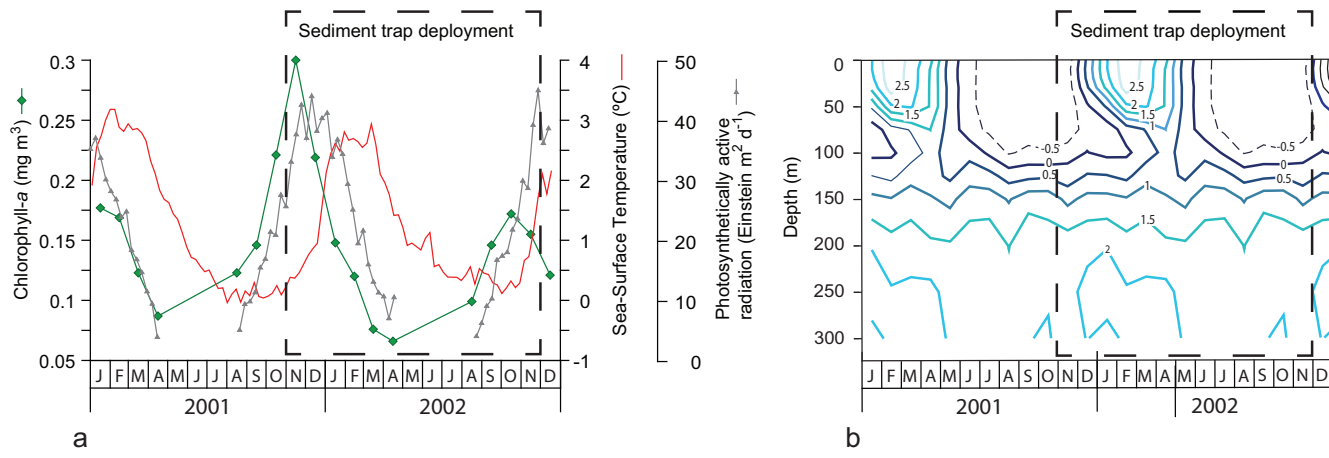
Figure 1
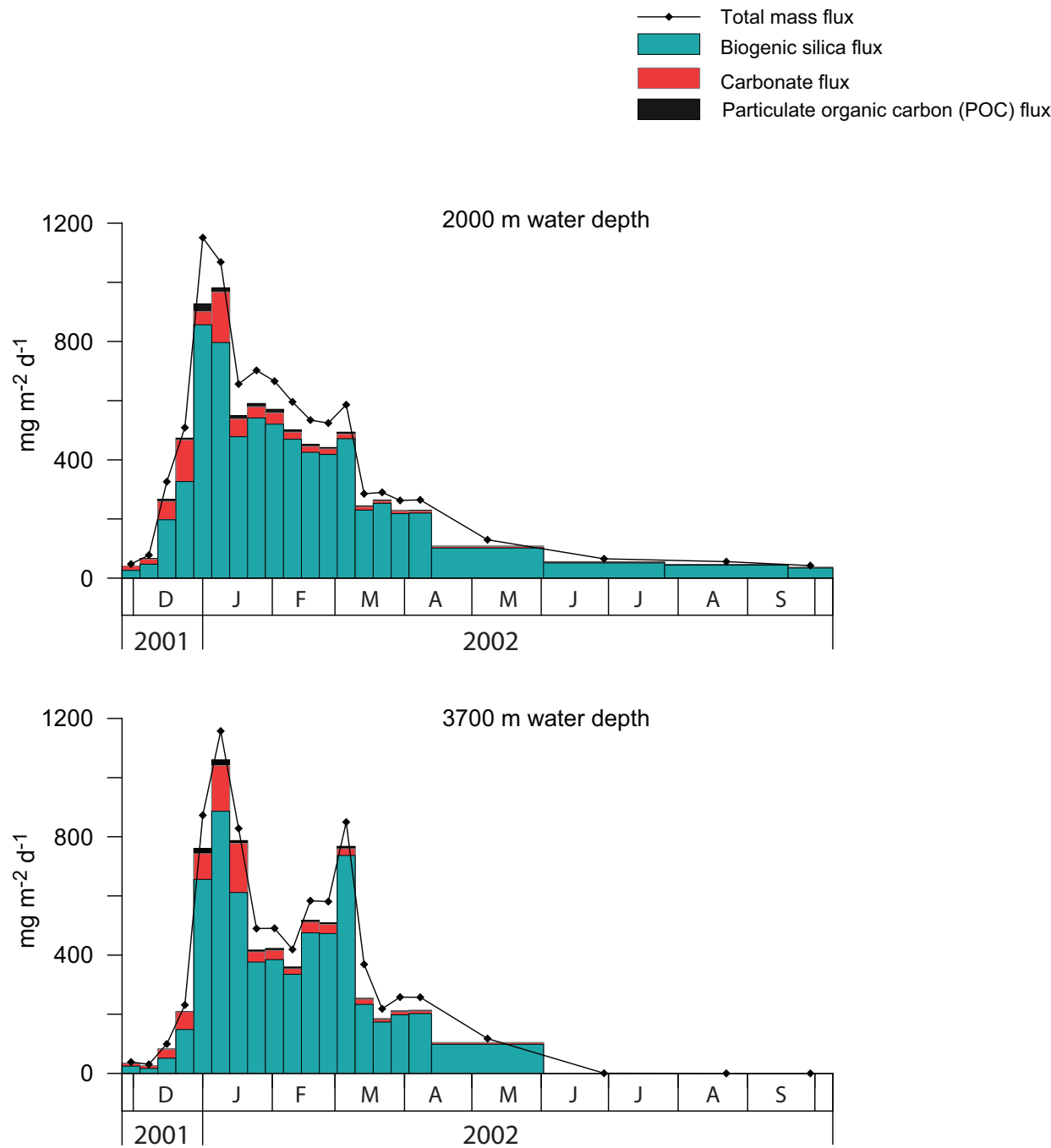
Figure 2

Figure 2

Figure 3

Figure 3

Figure 4

a

b

a

b

Figure 6